ELSEVIER

European Journal of Pharmacology 409 (2000) 243–257

ejp

www.elsevier.nl/locate/ejphar

Changes in intracellular Ca^{2+} by activation of P2 receptors in submucosal neurons in short-term cultures

Carlos Barajas-López [a,*], Rosa Espinosa-Luna [a], Fedias L. Christofi [b]

[a] *Department of Anatomy and Cell Biology, Queen's University, 9th Floor Botterell Hall, Kingston, ON, Canada K7L3N6*
[b] *Department of Anesthesiology, The Ohio State University, Columbus, OH, USA*

Received 31 July 2000; received in revised form 24 October 2000; accepted 31 October 2000

Abstract

Electrophysiological and Ca^{2+} microfluorimetric techniques were used to characterize the pharmacological profile of the P2 receptors expressed in submucosal neurons and the changes in intracellular Ca^{2+} associated with activation of these receptors. ATP caused a fast and slow membrane depolarizations during intracellular recordings. ATP induced a rapid inward current during whole-cell experiments. Receptors mediating the inward current and fast depolarization have the same pharmacological profile and these ATP responses were more sensitive to pyridoxalphosphate-6-azophenyl-2′,4′-disulfonic acid than Basilen BlueE-3G, and potentiated by suramin. The slow depolarization was not blocked by these P2 receptor antagonist, pertussis toxin, or KT5720 (protein kinase A inhibitor). *N*-ethylmaleimide or protein kinase C inhibitors (staurosporine and calphostin) blocked this depolarization. ATP induced complex multi-phasic Ca^{2+} transients in most neurons, classified as fast, slow, or mixed fast/slow responses. In conclusion, the fast and slow Ca^{2+} responses were mediated by respective activation of P2X and P2Y receptors and were associated with fast and slow depolarizations, respectively.

Keywords: Enteric neuron; Submucosal neuron; ATP receptor; Ca^{2+}; Receptor; P2X receptor; P2Y receptor; Ligand-gated channel

1. Introduction

In recent years, significant progress has been made in characterizing the membrane receptors and intracellular messengers transducing the signals for ATP. This has been fuelled, at least in part, by the recognition that ATP can play a role as a neurotransmitter in central and peripheral synapses. ATP release mediates excitatory junction potentials and smooth muscle contraction in some arteries, where it appears to be the main neurotransmitter (Burnstock, 1986; Evans and Surprenant, 1992). ATP has also been reported to mediate fast excitatory postsynaptic potentials in neuronal synapses of the rat habenula (Edwards et al., 1992), and cultured neurons from the guinea-pig coeliac ganglia (Evans et al., 1992; Silinsky and Gerzanich, 1993) or the myenteric plexus (Galligan and Bertrand, 1994).

Many neuromodulatory effects of ATP are mediated by its actions on P2X and P2Y receptors which are ligand-gated channels and G-protein-couple receptors, respectively. Interestingly, an increase in the cytosolic free Ca^{2+} concentration ($[Ca^{2+}]_i$) appears to play a key role in most biological responses to ATP. Thus, activation of P2Y-receptors is known to be often linked to phospholipase C signaling pathway leading to the mobilization of intracellular Ca^{2+} pools and a rise in $[Ca^{2+}]_i$. Activation of P2X receptors can also raise the intracellular Ca^{2+} by increasing the membrane Ca^{2+} influx through the P2X channels (which are permeable to extracellular Ca^{2+}) or through the voltage operated Ca^{2+} channels (which will open during ATP-evoked membrane depolarization).

In previous studies, we showed that ATP can induce two distinct depolarizations in S/type 1 submucosal neurons. The initial (fast) depolarization occurs concomitantly with a decreased in the membrane input resistance and it was suggested to be associated with the opening of ATP-gated cation channels (Barajas-López et al., 1994). The second depolarization (slow) occurs always associated with an increase in input membrane resistance and is mediated

* Corresponding author. Tel.: +1-613-533-2600; fax: +1-613-533-2566.
E-mail address: barajasc@meds.queensu.ca (C. Barajas-López).

0014-2999/00/$ - see front matter
PII: S0014-2999(00)00848-7

by inhibition of the membrane K^+ conductance (Barajas-López et al., 1994). It has been shown that the receptors mediating the fast and slow depolarizations have a different rank order of agonist potency and it is likely, although not proven, that they are mediated by activation of P2X and P2Y receptors, respectively (Barajas-López et al., 1993, 1994). The intracellular signal transduction mechanisms linked to these receptors in the submucosal neurons are also unknown. In contrast, it is known for myenteric neurons, that activation of P2Y receptors linked to the phospholipase C signaling pathway leads to a rise in $[Ca^{2+}]_i$ (Kimball et al., 1996; Christofi et al., 1997).

In the present study, we characterized the antagonist profile of the ATP receptors that mediate fast and slow membrane depolarizations in the submucosal neurons and investigated putative changes in the intracellular Ca^{2+} concentration associated with activation of these receptors.

2. Materials and methods

The microdissected submucous plexus preparation from the guinea-pig ileum was pinned to the Sylgard base of a recording chamber (capacity about 0.5–1 ml). An inverted microscope (×400; TMD, Nikon Canada Instruments, Mississauga, ON, Canada) was used to visualize the submucosal ganglia. Intracellular recordings were made with glass microelectrodes filled with 2–3 M KCl (resistance 60–100 M). Membrane potential was measured using an Axoclamp-2A preamplifier (Axon Instruments, Foster City, CA). The output of this preamplifier was displayed on an oscilloscope (Beckman 9020, Tucker Electronics, Garland, TX) and recorded with a PC and Axotape software (Axon Instruments). Classification of individual neurons was made according to previous criteria (Nishi and North, 1973; Hirst et al., 1974; Barajas-López et al., 1994): S/Type 1 neurons have fast nicotinic excitatory postsynaptic potentials and AH/Type 2 neurons show a long-lasting after hyperpolarization following a single action potential and no fast nicotinic excitatory postsynaptic potentials. Synaptic potentials were evoked as previously described (Barajas-López et al., 1995).

Submucosal preparations were continuously superfused with heated (35°C) physiological saline solution at 2–5 ml/min. This solution had the following composition (mM): NaCl 126, NaH_2PO_4 1.2, $MgCl_2$ 1.2, $CaCl_2$ 2.5, KCl 5, $NaHCO_3$ 25, glucose 11; gassed with 95% O_2 and 5% CO_2. Drugs were applied by superfusion or by pressure ejection. In the latter case, one or two pipettes (tip diameter 3–6 m) were filled with a solution of 2-chloroadenosine (1–5 mM), ATP (1–5 mM) or tetrodotoxin (1 μM) and pressure (typically 140 kPa for 10–250 ms) was used to eject a few nanoliters of these solutions on the ganglia containing the recorded cell, on the ganglion that was electrically stimulated or on the nerve strand between these two ganglia. To avoid unwanted effects due to leakage of the pipette solution, the pipette tip was always placed about 500 μm from the ejection site and was advanced up to the desired site, just before applying the solution. In some experiments, the neuronal cultures or submucosal preparations were maintained in growth medium containing 200–1000 ng/ml pertussis toxin during 24 h and 37°C.

2.1. Patch clamp recordings

Whole-cell currents were recorded from short-term (4–40 h) primary cultures of submucosal neurons from the guinea-pig ileum. Methods for dissociating and culturing submucosal neurons have been described elsewhere (Barajas-López et al., 1994, 1998). Briefly, the neurons were first dissociated using a papain solution (0.1 ml/ml; activated with 0.4 mg/ml of L-cysteine) and then with a collagenase (1 mg/ml) plus dispase (4 mg/ml) solution. After washing out these enzymes, the cells were plated on rounded coverslips coated with sterile rat tail collagen. Culture medium was minimum essential medium 97.5%, containing 2.5% guinea pig serum, L-glutamine 2 mM, penicillin 10 U/ml, streptomycin 10 μg/ml and glucose 15 mM.

Membrane currents were recorded using an Axopatch 1D amplifier. Patch pipettes were made as previously described (Barajas-López et al., 1994) and had resistances between 1 and 4 MΩ. With a typical pipette of 2 MΩ resistance and for maximal currents (usually no more than 2–4 nA), the voltage error due to series resistance would be lower than 10 mV, so in most cases, no compensation was made for this factor. The holding potential was usually −70 mV (range from −50 to −80 mV). Experiments were performed using the following solution inside the pipette (in mM): Cs-glutamate 160, EGTA 10, HEPES 5, NaCl 10, ATPMg 3 and GTP 0.1; adjusted to pH 7.4 with CsOH. The external solution had the following composition (in mM): NaCl 160, $CaCl_2$ 2, glucose 11, HEPES 5 and CsCl 3; the pH was adjusted to 7.3–7.4 with NaOH. With such solutions, the input resistance of the neurons ranged from 1 to 10 GΩ. When ATP concentrations higher than 100 μM were used to stimulate the cells the pH was readjusted with NaOH. Whole-cell currents were recorded with a PC using Axotape software (Axon Instruments). Membrane potentials were corrected for the liquid junction potentials (pipette 11 mV negative). Rapid changes in the external solution were made by using an eight-barrelled device (Barajas-López et al., 1994). ATP and its analogues were applied by abruptly changing the position of the tube, which delivered the external solution, in front of the recorded cell. Whole-cell experiments were performed at room temperature (~23°C).

2.2. Intracellular Ca^{2+} measurement

Submucosal neurons plated on 12 mm round coverslips were loaded with the Ca^{2+} membrane permeant indicator

1-[2-(5-carboxyoxazol-2-yl)-6-aminobenzofuran-5-oxyl]-2-(2′-amino-5′-methyl-phenoxy)-ethane-*N*,*N*,*N*′,*N*′-tetra-acetic acid penta-acetoxymethyl ester (fura-2/AM; 5 M). Loaded cells were placed in an incubator and gassed with 5% CO_2 for 45 min at 37°C, then rinsed once to remove excess dye, and allowed a 20 min postincubation at 37°C. This allowed complete hydrolysis of the membrane impermeant polycarboxylate anion (acid form of Ca^{2+} indicator). Coverslips with cells were mounted in a flow-through chamber (Biophysica Tissue Chamber) and placed on the stage of a Zeiss IM microscope system. Epifluorescence measurements from single cells isolated in the microscopic field were made using quartz optics and Zeiss Plan-Neofluor (63X) water-immersion objective for 5–10 min. The temperature of the buffer solution in the bath was maintained at 33°C, by passing the experimental solutions through a temperature controlled heat exchanger. The pH of the perfusate was maintained at about 7.4 by bubbling experimental solutions in reservoirs with 95% O_2/5% CO_2. Cells were excited by a 75-W Xenon lamp and a PTI photometry device at 340 and 380 nm, by using a computer-controlled reflective light chopper rotating at 50 or 250 Hz. Emissions (420–620 nm) were collected by photomultiplier tubes (Hammamatsu 928 PMT) and stored in the IBM-AT linked Deltascan system.

Neurons were briefly inspected for visual fluorescence through the binocular eye pieces, by setting the computer controlled shutter in the open position. A basal ratio (340/380 nm) of 2.2–3.0 was considered acceptable. The fluorescence measurements were restricted to the cell soma by adjusting the diaphragm to a fixed position to permit illumination of an area of ~35–40 μm. To avoid photobleaching of the cell, the computer-controlled shutter was closed when measurements were not being made.

Intracellular Ca^{2+} concentrations in fura-2/AM loaded neurons, were calculated from the ratio of the two excitation wavelengths (340/380 nm) as previously reported (Christofi et al., 1997) and according to the Grynkiewicz equation (Grynkiewicz et al., 1985): $[Ca^{2+}]_i = K_d \times [(R - R'_{min})/(R'_{max} - R)] \times (Sf2/Sb2)$. The determination of the apparent dissociation constant K_d, of fura-2 for Ca^{2+} proceeds from the equation: $K_d = EC_{50}/(Sf2/Sb2) = EC_{50}/B$, where Sf2 and Sb2 represent absolute fluorescence intensities at the excitation wavelength of 380 nm for the free and Ca^{2+}-saturated fura-2 dye. The Sf2 (380 nm) and Sb2 (380 nm) fluorescence intensities were obtained with pCa values of 8.0 and 4.0, respectively, during in vitro calibration performed at 33°C. An in vitro calibration curve was constructed by plotting fura-2 fluorescence ratios (340/380 nm) against varying *p*Ca concentrations (i.e., *p*Ca of 8.0 to *p*Ca of 4.0) utilizing a least squares analysis program (GraphPad, version 3.0) for nonlinear data. The EC_{50} of the sigmoidal calibration curve and the value for the calculated value for *B* were used to calculate the K_d. In vivo calibration on myenteric neurons was used to estimate R'_{max} and R'_{min} values, which represent the maximum and minimum fluorescence intensity ratios achievable in the cells. A concentration of 5 μM Bromo-A23187 was used to estimate the R'_{max} (Ca^{2+}-saturated) ratio. A 15-min incubation with Krebs solution containing 0 Ca^{2+} + 2 mM EGTA + a submaximal concentration of A23187 (0.5 μM) established the R'_{min} (Ca^{2+} free) ratio. Pooled values for both R'_{min} and R'_{max} were substituted into the original Grynkiewicz equation (Grynkiewicz et al., 1985) and the modified equation was used to convert ratios to Ca^{2+} concentrations. The response to 5 μM A23187

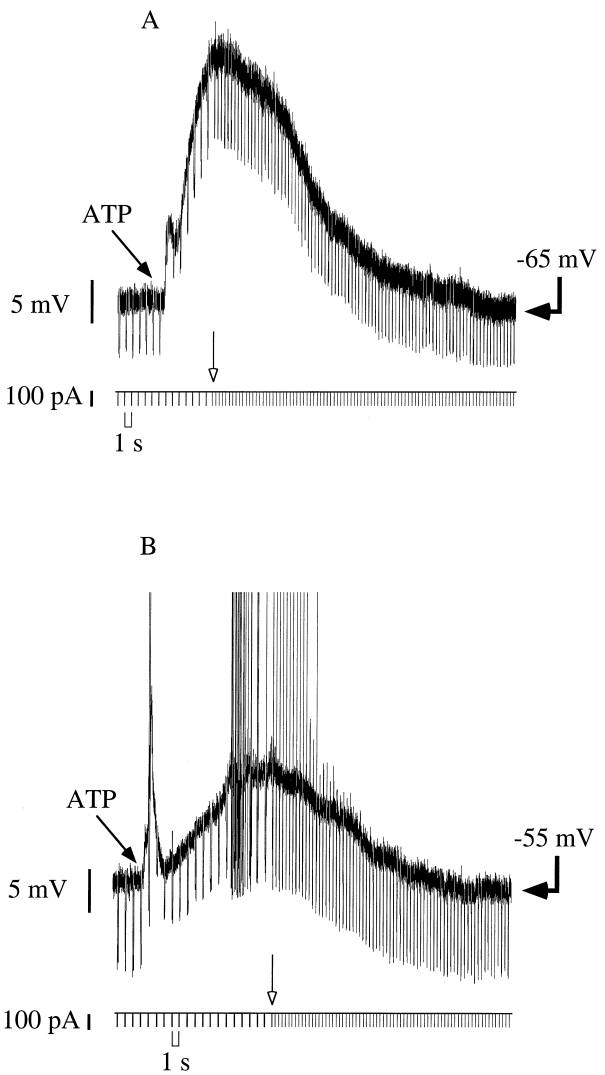

Fig. 1. Local application of ATP induced both a slow and a fast membrane depolarization in cultured submucosal neurons. A fast depolarization was always associated with a decrease in the amplitude of the electrotonic potentials, downward deflections of both upper panels, indicating a reduction in cell membrane input resistance. The subsequent slow depolarization was associated with an increase in membrane input resistance. Panels A and B are recordings from two different neurons. ATP was applied by pressure ejection using an ATP (5 mM) containing pipette, as indicated by a closed arrow. The open arrows indicate a change in the time calibration. Electrotonic potentials depicted in the lower trace of each panel were evoked by hyperpolarizing constant current pulses applied through the recording microelectrode.

was also routinely screened at the end of experiments to insure that R'_{max} did not change significantly from experiment to experiment, or as a result of a change in the photometer system.

2.3. Drug application

In Ca^{2+} experiments, ATP (5 mM) or adenosine-5′0 3-thiotriphosphate (ATP-γ-S; 2 mM) were applied by microejection from fine-tipped pipettes (tip diameter, 5 μm) with nitrogen pulses of controlled pressure and a duration of 0.5 s (Picospritzer, General Valve, East Hanover, NJ). The tips of the pipettes were positioned 100 μm from the recorded neuron. The superfusion solution for the Ca^{2+} experiments was modified Krebs Bicarbonate buffer containing (in mM): NaCl 125; KCl 1 mM; $CaCl_2$ 1.5; $MgCl_2$ 1.2; NaH_2PO_4 1.35; $NaHCO_3$ 14.4; glucose 12.7. The Krebs solution was warmed to 33°C and gassed with 95% O_2/5% CO_2 (pH 7.3–7.4). In all studies, the P2 receptor antagonists suramin or pyridoxalphosphate-6-azophenyl-2′,4′-disulfonic acid (PPADS) were applied by superfusion for 10-min periods. Staurosporine (3 μM) was applied for 20–30 min. Other inhibitors or drugs were applied for 10–15 min unless otherwise stated.

2.4. Drugs used

The following substances were purchased from Sigma (St. Louis, MO): Basilen BlueE-3G (dye concentration = 60%), adenosine 5′-triphosphate (ATP), adenosine deaminase, and pertussis toxin. Acetylcholine, 2-chloroadenosine, 8-cyclopentyltheophylline, *N*-ethylmaleimide, and pyridoxalphosphate-6-azophenyl-2′,4′-disulfonic acid (PPADS) from Research Biochemicals (Natick, MA). Suramin was purchased from Biomol Research Laboratories (Plymouth Meeting, PA). Staurosporine, calphostine, and KT5720 were purchased from Kamiya Biomedical (Thousand Oaks, CA). Fura-2/AM and Bromo-A23187 were purchased from Molecular Probes (Eugene, OR). Stock solutions of 0.1–10 mM were made in ethanol (8-cyclopentyltheophylline), dimethylsulphoxide (staurosporine, calphostine and KT5720), or in water (all other substances) prior to dissolving in the physiological saline solution. ATP stock solutions were prepared the day of the

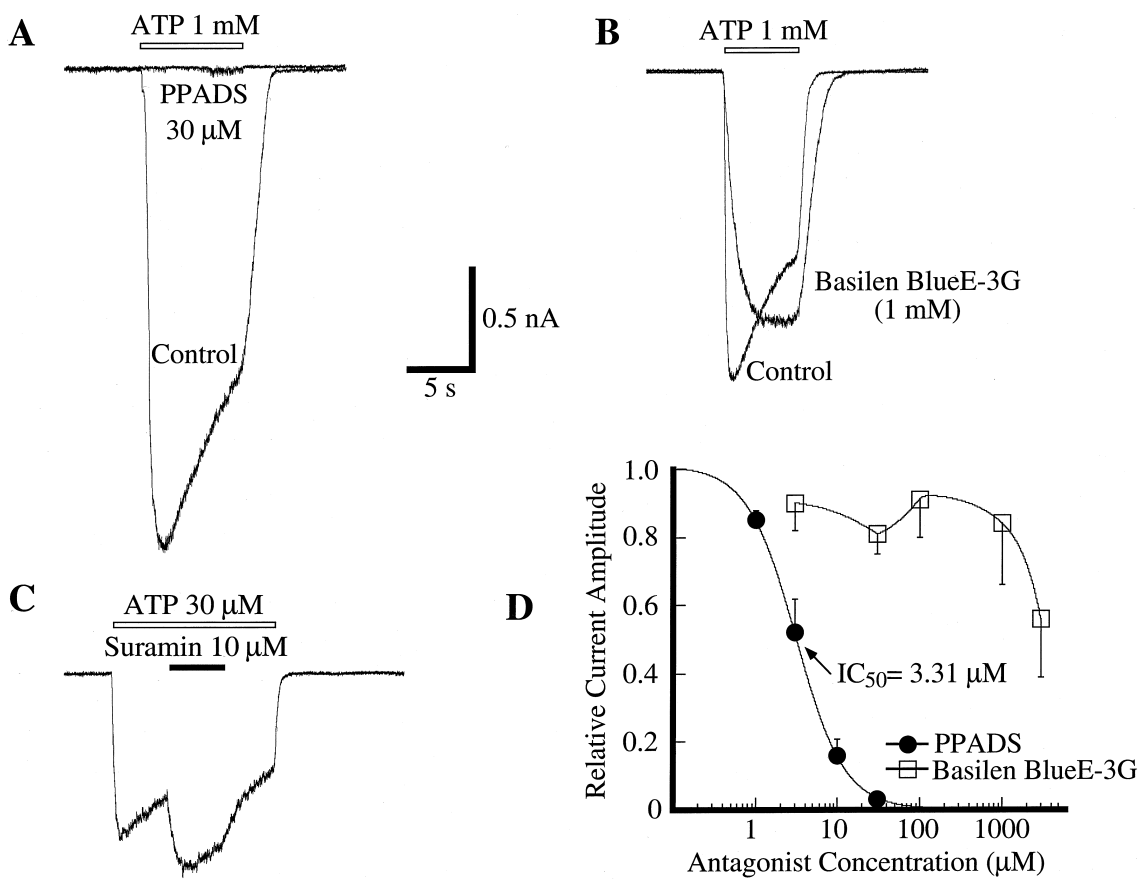

Fig. 2. Antagonist profile at P2X receptors of submucosal neurons. Whole-cell currents were elicited by ATP. (A) PPADS completely blocked the ATP-induced current. (B) Reactive blue increased the time to onset of the onset of the currents and partially blocked the ATP-induced currents. (C) The addition of suramin increased the amplitude of the ATP-induced current. Currents shown in A–C are from three different submucosal neurons and were measured at a holding potential of −60 mV. (D) Concentration–response curves for the effects of PPADS and Reactive Blue 2 on the inward current induced by 1 mM ATP. Symbols are means and vertical lines show S.E.M. (n = 3–5).

experiment. Stock solutions were kept at −4°C. Microejected drugs were at a concentration of 2–5 mM, pH 7.4, in Krebs solution. In experiments involving 0 $[Ca^{2+}]_o$ and 2 mM EGTA, the puff solution was made in modified Krebs solution containing 0 Ca^{2+}.

2.5. Data analysis

Results were expressed as means ± S.E.M. and the number of cells used as *n*. Data from Fig. 2 were fitted to a two-parameter logistic function as previously reported (Kenakin, 1993). Increases in $[Ca^{2+}]_i$ were calculated by subtracting the basal $[Ca^{2+}]_i$ in the unstimulated state from the total $[Ca^{2+}]_i$ obtained in the presence of drugs. Mean values ± S.E.M. of *n* experiments are reported. Statistical significance was inferred from P values = 0.05.

3. Results

3.1. General observations during intracellular experiments

As previously described (Barajas-López et al., 1994), the local application of ATP induced two distinct depolarizations in about ~70% of all S/type 1 submucosal neurons. In six analyzed experiments, in which a fast depolarization was clearly distinguished from the slow component, this component had a latency of 113 ± 12 ms, reached the peak in 0.9 ± 0.17 s, lasted for 3.5 s, and occurred concomitantly with a reduction in input resistance. The second component had a latency of 3 ± 0.9 s, reach the peak in 8.7 ± 2 s, lasted for 62 ± 14 s, was associated with an increase in input resistance, and a decrease in the membrane K^+ conductance.

The fast and slow depolarizations were also present in cultured submucosal neurons (Fig. 1). Twenty-two out of 25 recorded neurons responded to ATP local application. These neurons were recorded 4–10 days after the dissociation day and have a resting membrane potential of −58 ± 2 mV. Of the 22 neurons that responded to ATP, 10 showed a fast and a slow depolarization (Fig. 1), three only with a fast depolarization, and nine only a slow depolarization. In five out of the later nine neurons, the fast depolarization was unmasked after hyperpolarizing the cells close to the K^+ equilibrium potential (~ −95 mV), this maneuver annulled the slow depolarization (not shown), as previously shown in the submucosal preparation (Barajas-López et al., 1994). In 14 of 22 cells that responded to ATP, the fast and slow depolarizations were associated with action potentials (Fig. 1). The properties of these potentials was not investigated here because our sampling frequency was relatively low (1 kHz).

The observed differences in the kinetics of the slow and fast depolarizations are consistent with the hypothesis that

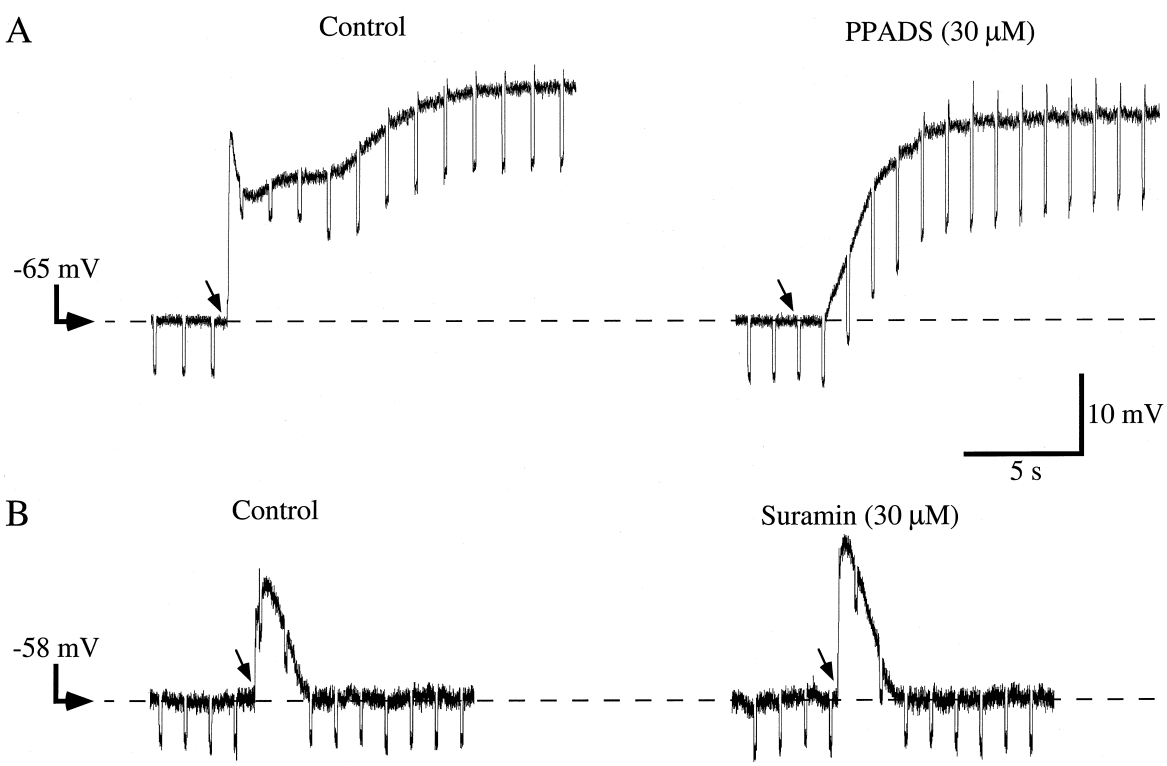

Fig. 3. The ATP-induced fast depolarization was inhibited by (A) PPADS and potentiated by (B) suramin. Note that both a slow and a fast depolarization are observed in the control recordings shown in panel A, whereas only a fast depolarization is observed in panel B; Panels A and B are recordings from two different neurons. Electrotonic potentials (fast downward deflections) were evoked by hyperpolarizing constant current pulses (0.1 pA) applied through the recording microelectrode. ATP was applied by pressure ejection as indicated by the arrow, using an ATP containing pipette (5 mM).

the fast response is mediated by the opening of ATP-gated channels (P2X) and the slow response by P2Y receptors.

3.2. P2X receptors mediate the ATP-induced fast depolarization in submucosal neurons

In a previous study, P2X receptors were shown to be present in about 78% of submucosal neurons, and the rank-order of potency of ATP and other analogs to activate these receptors was: ATP = ATP-γ-S = 2-Me-S-ATP ≫ β,γ-methylene ATP = α.β-methylene ATP (Barajas-López et al., 1994). Note that in such study, P2X receptors of submucosal neurons were classified as P2Y in agreement with their agonist profile and the previous classification of P2 receptors (Fredholm et al., 1994; Kennedy and Leff, 1995). In this study, we determined the antagonistic profile at these receptors.

PPADS (1–30 μM; $n = 11$) inhibited the whole-cell inward currents induced by ATP (1 mM) in a concentration-dependent manner (Fig. 2A and D). In 11 cells, the control value of these currents was -1755 ± 250 pA, which was reduced to -53 ± 10 pA in the presence of 30 μM of PPADS. The onset of this PPADS action was relatively slow and therefore, its effects were measured 5 min after (steady state) starting its superfusion, when the maximal effect was reached. The response to PPADS was washed out very slowly; ATP-activated currents were $20 \pm 4.0\%$ ($n = 5$) and $50 \pm 5.5\%$ ($n = 3$) of their control amplitudes 5 and 15 min after terminating PPADS superfusion. PPADS did not affect the inward currents induced by

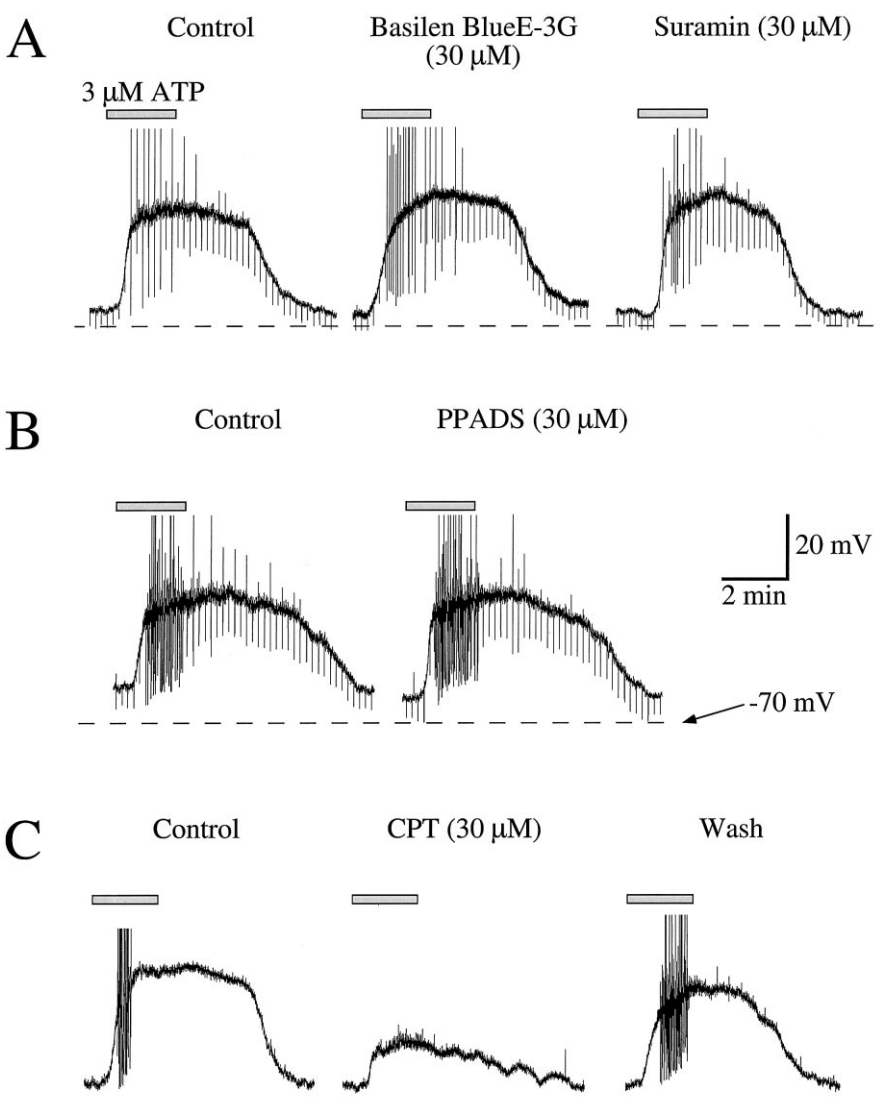

Fig. 4. The P1 receptor antagonist 8-cyclopentyltheophylline (CPT) reduced the amplitude of the ATP-induced slow membrane depolarization but not the P2 receptor antagonists, Basilen BlueE-3G, suramin, or PPADS. Dashed lines represent the indicated membrane potential (−70 mV). All three panels (A–C) are recordings from two different neurons and ATP was applied by superfusion as indicated by bars.

acetylcholine (30 μM). The control acetylcholine response which had a mean value of -775 ± 110 pA ($n = 4$), remained the same (-783 ± 108 pA) in the presence of PPADS (30 μM; $n = 4$). No change in the whole-cell holding current was induced by PPADS (30 μM).

Application of Basilen BlueE-3G (Reactive Blue 2; 3–3000 μM; $n = 4$) only partially decreased the whole-cell inward currents induced by ATP (1 mM) whereas it did not induce any change in the holding current. The maximal concentration of Basilen BlueE-3G used, decreased the ATP induced current by $56 \pm 17\%$ of its control value (Fig. 2B and D). Moreover, the onset of the ATP-induced current was significantly slowed down by Basilen BlueE-3G; thus, the time required to reach the half-maximal current increased in the presence of 100 μM Basilen BlueE-3G from 145 ± 12 to 698 ± 37 ms ($n = 4$). The effects of this dye were measured 3–5 min after application and were fully reversed 10–20 min after their washout.

Suramin (10–30 μM) fail to inhibit the whole-cell inward currents induced by ATP. Indeed, a potentiation of the ATP effects was observed in 12 out of 14 cells (Fig. 2C). This potentiation was reversible, and occurred when suramin was applied either before (1–10 min; $n = 5$) or during ATP stimulation ($n = 7$). In five experiments, the currents induced by ATP (10 μM) were significantly ($P < 0.01$) increased by the addition of suramin (30 μM),

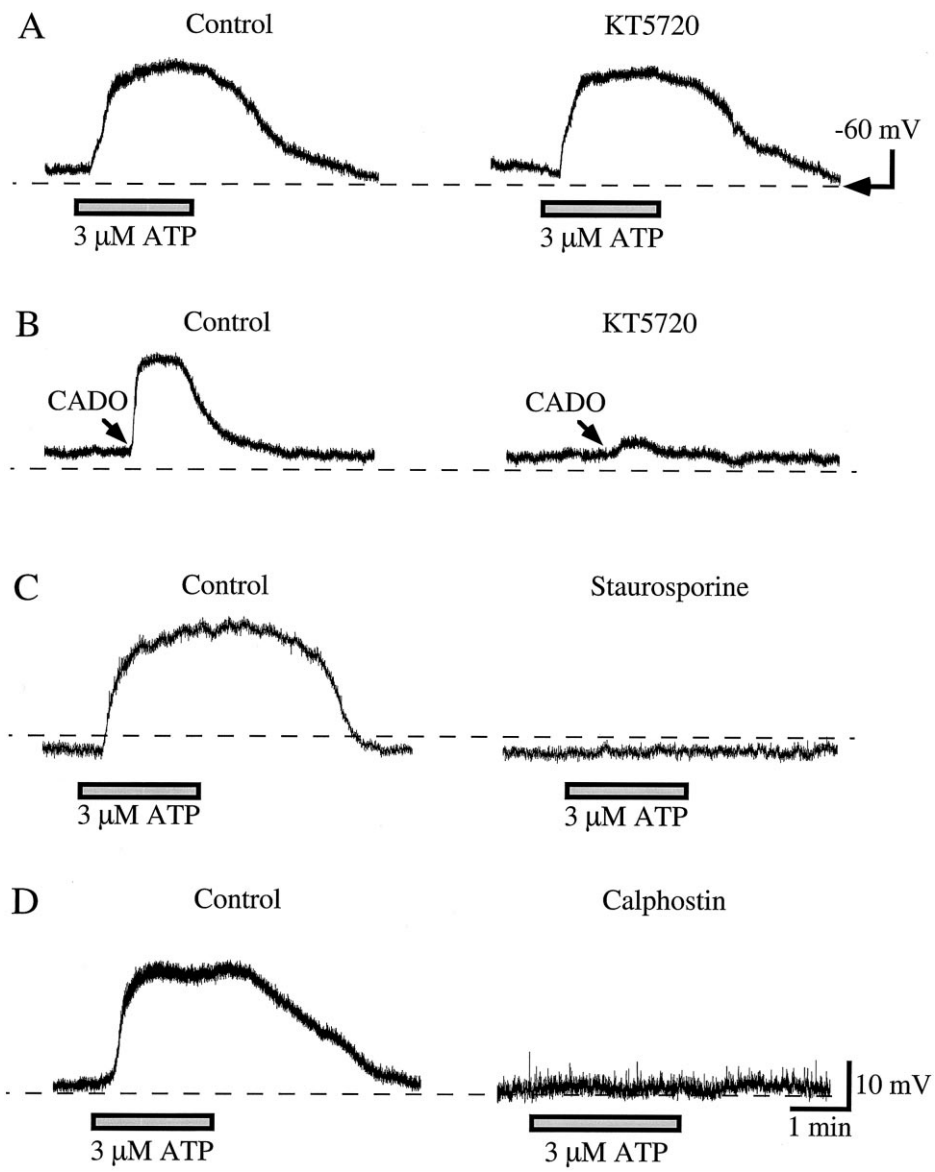

Fig. 5. The ATP-induced slow depolarization might involve protein kinase C activity. KT5720 (a protein kinase A inhibitor) did not alter this ATP response but inhibited that slow depolarization induced by the adenosine receptor agonist, 2-chloroadenosine (CADO). Staurosporine or calphostin (two protein kinase C inhibitors) suppressed the ATP-induced slow depolarization. The dashed line indicates the indicated membrane potential (−60 mV). Panels A and B are recordings from the same neuron, whereas panels C and D are from two different neurons. ATP was applied by superfusion as indicated by bars (A, C and D) whereas the P1 receptor agonist 2-chloroadenosine was applied by pressure ejection (as indicated by the arrow; B).

with mean currents of -435 ± 135 and -595 ± 85, respectively. Suramin alone (up to 1 mM) did not change the holding current, which had a value of 20 ± 8 pA in four analyzed cells. Nicotinic currents induced by acetylcholine (30 μM, -725 ± 103) were also not modified by suramin (100 μM, -720 ± 105 pA) and ($n = 5$). These observations would imply that suramin acts on a regulatory mechanism specific to ATP-gated channels to potentiate the effects of ATP, as it was proposed in myenteric neurons (Barajas-López et al., 1996a).

In intracelular studies, we demonstrated that PPADS (30 μM) significantly inhibited the fast depolarization induced by ATP. The ATP-induced depolarization in submucosal neurons was reduced from 23 ± 0.9 to 3 ± 2.8 mV by PPADS ($n = 4$; $P < 0.01$; Fig. 3A); no difference was evident between responses in cultured neurons and neurons in intact preparations. The effect of suramin on the fast depolarization was also tested in four cultured neurons and in four neurons of intact submucosal preparations. In six of these eight neurons, suramin significantly increased the amplitude of the fast ATP depolarization from 15.0 ± 1.5 and 20 ± 1.8 mV ($P < 0.05$, see representative Fig. 3B). No change was observed in the other two neurons.

3.3. P2Y receptors mediated the ATP-induced slow depolarization in submucosal neurons

The rank-order of potency of ATP and its analogs to induce the slow depolarization was previously described (Barajas-López et al., 1994) and this was: 2-methylthio-ATP (2-Me-S-ATP) > ATP > ATP-γ-S = ADP; α,β-methylene ATP, and β,γ-methylene ATP were inactive (10–100 μM). In the present study, we first investigated the effects of PPADS (30 μM), Basilen BlueE-3G (30 μM), and suramin (30 μM) on the slow depolarization induced by ATP.

None of these P2 receptor antagonists have any effect on the resting membrane potential or on the slow depolarization induced by 3 μM ATP (Fig. 4A–B). The mean control amplitudes of this depolarization in three cell groups treated with these substances were 31 ± 2.7 ($n = 3$), 33 ± 2.5 ($n = 3$) and 23 ± 2.3 ($n = 5$) mV, and in their presence were 30 ± 4.1, 31 ± 4.5 and 28 ± 5.1 mV, respectively.

8-Cyclopentyltheophylline (30 μM) reduced the ATP-induced slow depolarization from its control value of 22 ± 2.8 to 12 ± 1.4 mV ($P < 0.05$; $n = 5$; Fig. 4C). At 10 μM concentration, 8-cyclopentyltheophylline did not affect the ATP-induced slow depolarization; the respective values for the ATP response before and after 8-cyclopentyltheophylline were 27 ± 2.6 and 29 ± 2.5 mV ($n = 5$). 8-Cyclopentyltheophylline also did not alter the resting membrane potential at any of the used concentrations.

To investigate if the ATP metabolite, adenosine, was mediating part of the ATP-induced depolarization, we studied the effect of the enzyme adenosine deaminase (2 U/ml) and α,β-methylene ADP (50 μM) on the slow depolarization induced by 3 μM ATP. Superfusion of these substances was initiated 3–5 min before adding ATP and maintained as long as the ATP superfusion. These experiments were performed with an ATP stock solution (10 mM concentration) that had been pre-incubated with 10 U/ml of adenosine deaminase for 1–6 h. We found that the simultaneous superfusion of adenosine deaminase and α,β-methylene ADP neither altered the resting membrane potential nor the ATP-induced slow depolarization. The value of the depolarization before (23 ± 2.7 mV) and after treatment (23 ± 1.9 mV) remained the same ($n = 5$). In our hands, the same concentration of adenosine deaminase was able to completely abolish the adenosine-induced presynaptic inhibition of acetylcholine release in the submucosal plexus (Barajas-López et al., 1995).

The following experiments were carried out to investigate the putative involvement of G-proteins and protein phosphorylation in the slow depolarization induced by ATP (3 μM). It was found that KT5720 (a protein kinase A inhibitor; 3 μM) did not block this depolarization, control values were 19 ± 2.6 mV and in the presence of this substance 18 ± 2 mV ($n = 3$; Fig. 5A). In the same cells, however, KT5720 did inhibit the slow depolarization

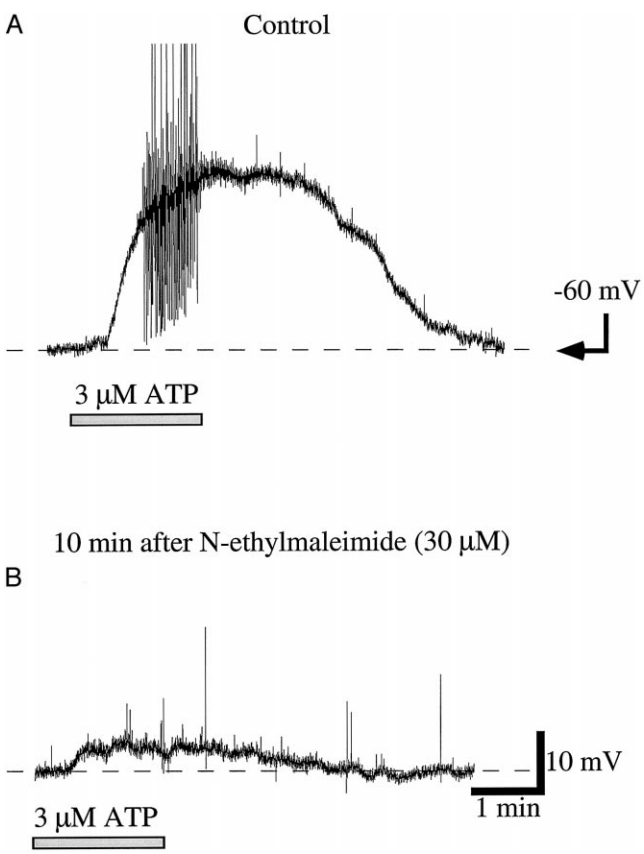

Fig. 6. *N*-ethylmaleimide significantly decreased the ATP-induced slow depolarization. The dashed line indicates the membrane potential. Both recordings are from the same neuron, before (A) and 10 min after (B) initiating *N*-ethylmaleimide superfusion.

induced by 2-chloroadenosine (Fig. 5B). However, staurosporine (Fig. 5C) or calphostin (Fig. 5D) significantly abolished the ATP-induced slow depolarization (3 μM; $n = 3$ for each; $P < 0.05$). Control mean values were 21 ± 4 and 20 ± 3.5 mV, whereas 15 min after starting the superfusion of these protein kinase inhibitors this depolarization was 3 ± 1.5 and 6 ± 1.5 mV, respectively.

On the other hand, *N*-ethylmaleimide (10–30 μM; a substance that can uncouple receptors from G-proteins) significantly reduced the slow depolarization induced by ATP (3 μM; Fig. 6) from 25 ± 0.8 to 7 ± 2.1 mV ($n = 6$; $P < 0.001$) after superfusion of *N*-ethylmaleimide for 10 min. This effect of *N*-ethylmaleimide was irreversible. This substance, however, did not modify the resting membrane potential or the input membrane resistance of these neurons.

Pretreatment of submucosal preparations with pertussis toxin (G_i/G_o inhibitor) did not change the slow depolarization induced by ATP (3 μM), which had a value of 23 ± 2.0 mV in six neurons; such a value of depolarization is similar to that obtained in untreated cells.

3.4. Effects of P2 receptor agonists on intracellular free Ca^{2+} levels

Our previous studies showed that ATP acts mainly at P2 receptors to elevate $[Ca^{2+}]_i$ in myenteric neurons of the small bowel (Christofi and Wood, 1994; Christofi et al., 1997). In this study, ATP, as well as its analog ATP-γ-S, caused a transient rise in $[Ca^{2+}]_i$ in single cultured submucosal neurons. A total of 56 of 81 neurons (70%) from 21 cultures prepared from the submucosal plexus of the small bowel (i.e., six animals used), responded to ATP with a Ca^{2+} transient.

3.5. Temporal analysis of purinergic Ca^{2+} transients by photometry

Several distinct ATP Ca^{2+} profiles were obtained in submucosal neurons (Fig. 7). Submucosal neurons displayed three types of Ca^{2+} responses with significantly different kinetics. Responses were classified as fast (i.e., latency < 1.0 s, Fig. 7A and B), slow (i.e., latency > 2.0

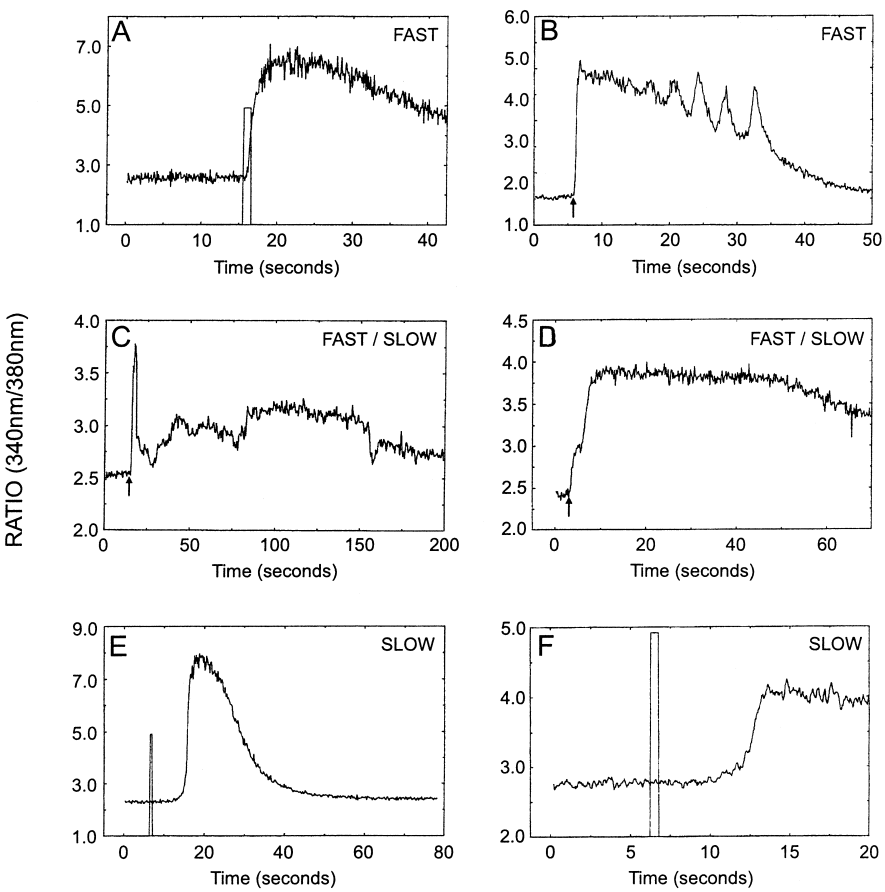

Fig. 7. Submucosal neurons display three types of ATP Ca^{++} transients. (A) Fast ATP Ca^{2+} transient with a latency < 1.0 s. (B) Fast ATP Ca^{2+} transient with Ca^{2+} oscillations which occurred following the initial fast rise in $[Ca^{2+}]_i$. (C) Neuron displaying an initial fast response (latency < 1.0 s) followed by a slow response (latency > 10 s). (D) Another example of a mixed fast/slow response. (E, F) Examples of neurons displaying only a slow response (latency > 5 s). ATP (5 mM, pH 7.4) was applied by pressure microejection for 1.0 s. Basal $[Ca^{2+}]_i$ values: (A) 63 nM; (B) 61 nM; (C) 63 nM; (D) 70 nM, (E) 62 nM, (F) 102 nM. Peak ATP $[Ca^{2+}]_i$ values: (A) 1347 nM; (B) 575 nM; (C) fast response = 257 nM and slow response = 203 nM; (D) fast response = 162 nM and slow response = 321 nM.

s, Fig. 7E and F), or those in which the initial fast response was followed by a slow response in the same neuron after a single "puff" of ATP (see Fig. 7C and D). Complex multiphasic Ca^{2+} transients were also observed in the neurons (Fig. 7B and C). The magnitude of the ATP Ca^{2+} transients varied significantly between different neurons in culture. The characteristics of the ATP Ca^{2+} responses are reported in Table 1. Significant differences were observed between fast and slow ATP responses in terms of the kinetics and t_{peak}. However, no difference was apparent between either the duration or the magnitude of peak Ca^{2+} responses of fast and slow ATP Ca^{2+} transients, and such data were therefore pooled together for both types of responses. The basal level of $[Ca^{2+}]_i$ in cultured submucosal neurons was 79.6 nM ($n = 13$). The peak Ca^{2+} response to local application of ATP (5 mM) on single cultured submucosal neurons was 728.7 nM ($n = 13$). The average duration of the ATP Ca^{2+} transients was 65.2 s ($n = 13$).

3.6. Pharmacological characterization of fast Ca^{2+} transients

Further studies focused on the pharmacology of fast Ca^{2+} transients in cultured submucosal neurons. The results are summarized in Table 2. Omission of Ca^{2+} from the superfusion solution reversibly reduced the peak ATP Ca^{2+} response by about 80% (Fig. 8A). Further inclusion of the extracellular Ca^{2+} chelator EGTA (2 mM) abolished the ATP response (Fig. 8B). The P2 receptor antagonist suramin, enhanced the ATP Ca^{2+} transient. Enhancement was observed as an increase in the peak Ca^{2+} response, as well as a significant delay in the $t_{1/2}$ recovery of the ATP Ca^{2+} transient (see Fig. 9A and B) that ranged from 80% to 120%. In the absence of extracellular Ca^{2+} (i.e., 0 Ca^{2+} 2 mM EGTA), the suramin-enhanced ATP response was also abolished (see Fig. 9B). The identical result was obtained in two additional experiments. The more specific P2 receptor antagonist PPADS always blocked or prevented the fast ATP Ca^{2+} response (Table 2, Figs. 9A and 10B). In three experiments in which both suramin and PPADS were tested on the same submucosal neuron, suramin enhanced and PPADS always antagonized the ATP Ca^{2+} response (see Fig. 9A). Blockade of voltage operated Ca^{2+} channels with 100 μM Cd^{2+} reversibly reduced but never abolished the ATP Ca^{2+} response. Cd^{2+} apparently reduced the initial fast rising component of the response (see Fig. 10A and B). Staurosporine had no

Table 1
Kinetics of ATP Ca^{2+} transients in submucosal neurons

ATP response	n	Latency	t_{peak} (s)
Fast	21	0.45 ± 0.07	3.63 ± 0.46
Slow	12	6.2 ± 1.10	7.32 ± 1.91
Fast/slow	9	N/C	N/C

Difference between latencies of fast and slow responses was $P < 0.0001$; difference between t_{peak} response of fast and slow responses was $P = 0.0142$. Mann–Whitney U-statistics, two-tail P values are reported. N/C, not calculated.

Table 2
Pharmacology of the ATP-induced fast Ca^{2+} transients in culture submucosal neurons

Treatment	n	Percentage change in Ca^{2+} response	Effect
0 Ca^{2+}	4	−82.5 ± 3.0	Inhibition
0 Ca^{2+} plus 2 mM EGTA	6	−99.0 ± 1.8	Inhibition
Suramin, 30 μM	7	+82.3 ± 11.3	Potentiation[a]
PPADS, 30 μM	10	−93.1 ± 5.1	Inhibition
Cd^{2+}, 100 μM	5	−60.0 ± 5.5	Inhibition
Staurosporine, 3 μM	6	−10.5 ± 4.9	No effect

[a] For suramin, potentiation was calculated as the percentage increase in the half-recovery time ($t_{1/2}$ recovery) from peak Ca^{2+} response.

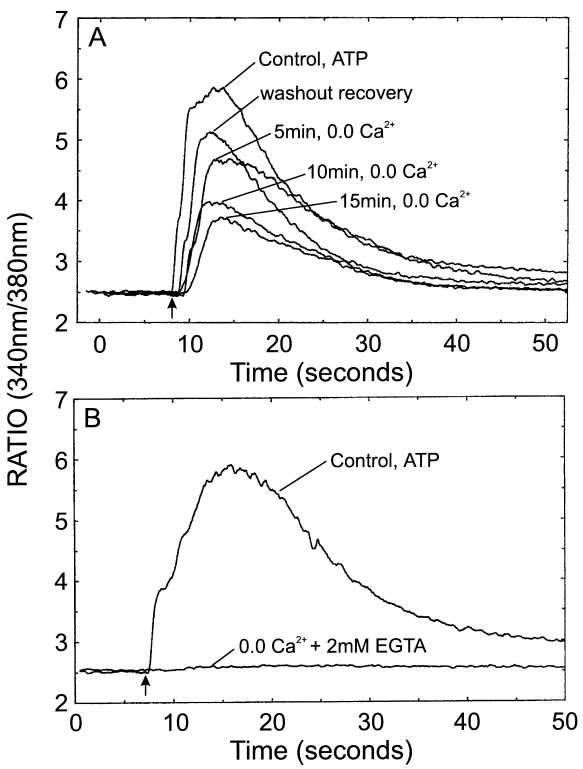

Fig. 8. Contribution of Ca^{++} influx to the fast ATP Ca^{++} transients in submucosal neurons. (A) Omission of Ca^{2+} from the bathing solution reduced the peak ATP Ca^{2+} response in a time-dependent and reversible manner. The ATP Ca^{2+} response recovered when the Ca^{2+} concentration was restored to 1.5 mM for 15 min. (B) In a different submucosal neuron, the ATP Ca^{2+} transient was abolished when the bathing solution was modified to include 2 mM EGTA and 0 Ca^{2+}. Basal $[Ca^{2+}]_i$ levels: (A) 70 nM; (B) 81 nM. Peak ATP $[Ca^{2+}]_i$ values: (A) Control ATP, 719 nM; 5 min 0 Ca^{2+}, 463 nM; 10 min 0 Ca^{2+}, 306 nM; 15 min 0 Ca^{2+}, 248 nM; washout recovery, 575 nM. (B) Control ATP, 690 nM; 0 Ca^{2+} + 2 mM EGTA, 85 nM.

clear and consistent effect on the shape of the ATP Ca^{2+} transient, and never inhibited the response (see Fig. 10C). In two cells, staurosporine prolonged the plateau phase of the fast ATP response. In three experiments in which PPADS blocked more than 90% of the response, Cd^{2+} reduced the response, but staurosporine did not block the response (see Fig. 10B).

3.7. Pharmacology of slow Ca^{2+} transients

An attempt was made to further characterize the pharmacology of 'slow' Ca^{2+} transients, but this proved to be a much more difficult task, because these responses were less frequent, and also it was more difficult to reproduce them multiple times which is needed to test various blocking agents. In three neurons, 'slow' ATP Ca^{2+} transients were not blocked by PPADS (30 μM). In another four neurons, the ATP response was reduced or abolished by 30 μM *N*-ethylmaleimide. Inhibition of voltage operated Ca^{2+} channels by 100 μM Cd^{2+} failed to block the slow response ($n = 3$).

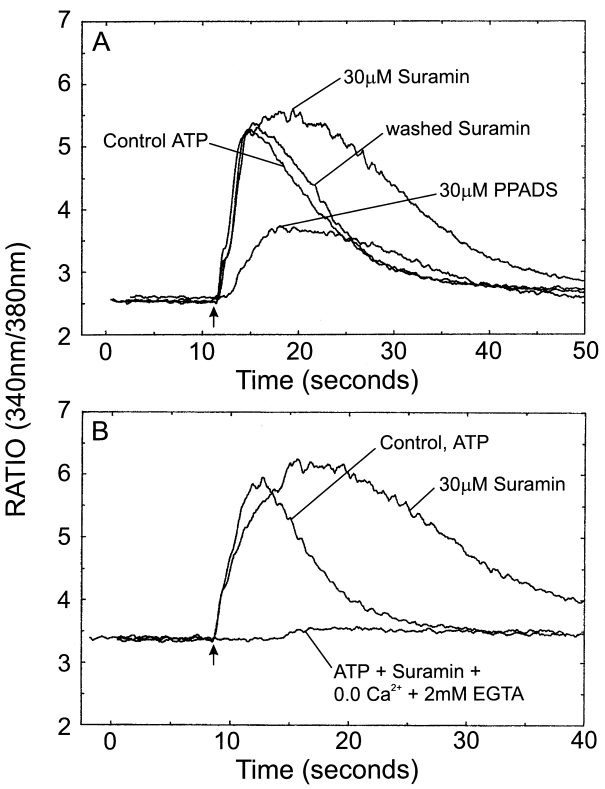

Fig. 9. Suramin potentiates the fast ATP Ca^{++} response in submucosal neurons. (A) Suramin increase the peak ATP-induced Ca^{2+} response, as well as an increase in the half time of recovery ($t_{1/2} = 105\%$). Following a 10-min washout recovery from suramin. PPADS, another P2 receptor antagonist, suppressed the ATP Ca^{2+} response. (B) In another neuron, suramin potentiated the ATP Ca^{2+} response and this was abolished by removal of extracellular Ca^{2+}. Neurons were treated with suramin or PPADS for 10 min. Basal $[Ca^{2+}]_i$ levels: (A) 70–75 nM; (B) 151 nM. Peak ATP $[Ca^{2+}]_i$ values: (A) Control ATP, 604 nM; 30 μM suramin, 651 nM; washed suramin, 610 nM; 30 μM PPADS, 241 nM. (B) Control ATP, 740 nM; 30 μM suramin, 886 nM; suramin + 0 Ca^{2+} + 2 mM EGTA, 201 nM.

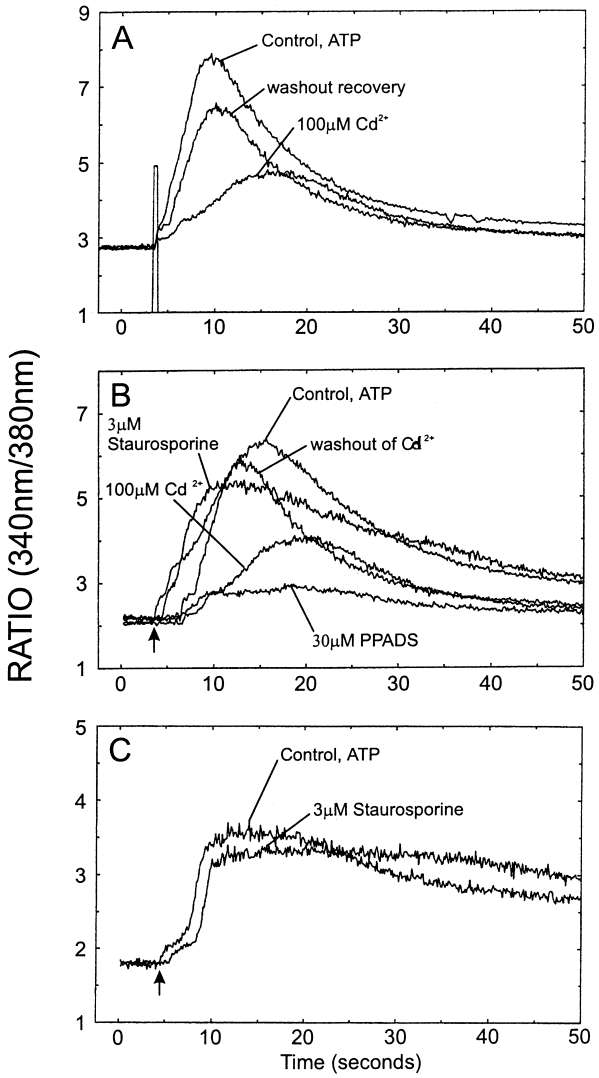

Fig. 10. The fast P2 receptor-mediated rise in $[Ca^{++}]_i$ in submucosal neurons involves activation of voltage activate Ca^{++} channels but not protein kinase C. As it is shown in (A) and (B), Cd^{2+} reduced the ATP Ca^{2+} responses in two different neurons. (B) Subsequent treatment with PPADS antagonized this response (the recovery response to PPADS is the same as that for washout of Cd^{2+}). Staurosporine did not inhibit the ATP response in the same neuron (B) or in a naive neurons (C). Basal $[Ca^{2+}]_i$ levels: (A) 104 nM; (B) 65 nM; (C) 52 nM. Peak ATP $[Ca^{2+}]_i$ levels: (A) Control ATP (5 mM), 1492 nM; 100 μM Cd^{2+}, 427 nM; washout recovery, 908 nM. (B) Control ATP (5 mM), 881 nM; 100 μM Cd^{2+}, 284 nM; washout of Cd^{2+}, 719 nM; 3 μM staurosporine, 629 nM; 30 μM PPADS, 154 nM. (C) Control ATP (2 mM), 240 nM; 3 μM staurosporine, 220 nM.

4. Discussion

Our results indicate that ATP induces fast and slow depolarizations in submucosal neurons by interacting with P2X (ligand-gated channels) and P2Y (G-protein linked)

receptors, respectively. These two populations of receptors have different pharmacological properties and their activation is associated with a rise in $[Ca^{2+}]_i$. Activation of P2X receptors leads to an increase in what likely results from Ca^{2+} influx through both P2X channels and voltage operated Ca^{2+} channels. Activation of P2Y receptors is associated with a slower rise in $[Ca^{2+}]_i$. Our data indicate that Ca^{2+} is likely to be a major intracellular signal for transduction of both P2X and P2Y purinergic messages in submucosal neurons.

4.1. Fast depolarization

In a previous study, we have shown that the fast inward current induced by ATP is mediated by the opening of cation-nonspecific ion channels, which by definition are P2X receptors (Barajas-López et al., 1994). Several observations indicate that the ATP-induced fast depolarization is also mediated by activation of P2X receptors. First, the amplitude of this depolarization, as the amplitude of the inward current, is increased by hyperpolarizing the submucosal neurons (Barajas-López et al., 1994). Second, the membrane conductance increased during both, the fast depolarization and the inward current (Barajas-López et al., 1994). Finally, the agonist (Barajas-López et al., 1994) and the antagonist (present study) profiles for both the depolarization and the inward current were virtually the same.

P2X receptors expressed on myenteric (Barajas-López et al., 1996a) and submucosal neurons have an unusual pharmacological profile. The existence of a complex population of P2X receptors was initially suspected by the observation that the non-hydrolysable ATP-analog α,β-methyleneATP behaves as a full agonist in some neurons whereas it has little or no agonist action in others (Friel, 1988; Friel and Bean, 1988; Fieber and Adams, 1991; Bean, 1992; Kennedy and Leff, 1995; Khakh et al., 1995). In agreement with this early interpretation, seven P2X receptor cDNAs have been cloned (see references by North, 1996; Collo et al., 1997). One of the major pharmacological differences between these subtypes appears to be in the absolute EC_{50} values for ATP and α,β-methyleneATP. Thus, the P2X1 and P2X3 receptors are activated by high nanomolar to low micromolar concentrations of these two agonists. The other four receptors, P2X2, P2X4, P2X5, and P2X6, are activated by low micromolar concentrations of ATP but relatively high concentrations of α,β-methyleneATP (>100 μM). The agonist profile of the submucosal P2X receptor is similar to P2X4 and P2X6 receptors, and is therefore, activated by low micromolar concentrations of ATP and insensitive to the agonist α,β-methyleneATP (Barajas-López et al., 1994). However, the P2X receptors on submucosal neurons differ in some respects from P2X4 and P2X6 subtypes. In this regard, ATP-γ-S is a full agonist and as potent as ATP at the submucosal P2X receptor (Barajas-López et al., 1994), whereas it is a partial agonist at the P2X6 (Collo et al., 1996) and less potent than ATP at the P2X4 (Buell et al., 1996). Furthermore, there are significant differences in the antagonist profile of these three receptors. PPADS, for instance, is an effective antagonist at the submucosal P2X receptor (present study) but is reported to have no effect at the P2X4 or P2X6 receptors (Buell et al., 1996; Collo et al., 1996; Soto et al., 1996). Suramin potentiates the ATP actions at the submucosal P2X receptor (present study) whereas this response does not occur at the P2X4 or P2X6 (Buell et al., 1996; Collo et al., 1996; Soto et al., 1996). Therefore, it is clear that the native submucosal P2X receptor shares only some properties with the P2X receptors so far characterized molecularly, and in particular with the P2X4 or P2X6 receptors. This indicates that it may represent a novel functional subtype of P2X receptors. Another possibility, however, is that P2X submucosal channels are the result of the combination of two or more of the six homomeric receptors so far characterized. In agreement with the latter interpretation, it has been proposed that at least some native P2X receptors could be made up of heteromultimers (Lewis et al., 1995).

The antagonist profile of submucosal P2X receptors is similar to those of myenteric P2X receptors (Barajas-López et al., 1996a) but different than other existing neuronal native P2X receptors. Thus, reactive blue 2 had a very weak antagonistic effect ($IC_{50} > 3$ mM) on P2X submucosal receptors, whereas it has been shown to block, rather potently ($K_d = 1–6$ μM) the actions of ATP at P2X receptors of other neurons (Fieber and Adams, 1991; Silinsky and Gerzanich, 1993; Nutter and Adams, 1994; Khakh et al., 1995). A prominent pharmacological property of enteric (submucosal and myenteric) P2X receptors is that suramin potentiated ATP effects whereas it inhibited ATP actions on these receptors in central (Edwards et al., 1992; Inoue et al., 1992) and peripheral neurons (Evans et al., 1992; Silinsky and Gerzanich, 1993; Khakh et al., 1995). PPADS was the only effective antagonist for enteric P2X receptors (present study and (Barajas-López et al., 1996a) as it has been shown for other P2X receptors (Connolly, 1995; Windscheif et al., 1994; Valera et al., 1994).

4.2. Slow depolarization

In a previous study, we showed that the slow depolarization induced by ATP is mediated by a decrease in the K^+ membrane conductance and we proposed the involvement of a diffusible intracellular messenger in this response (Barajas-López et al., 1994). Several observations of the present study are in agreement with such a hypothesis and suggest that the ATP receptor mediating the slow depolarization is a member of the large family of G protein-couple receptors and therefore a P2Y receptor, according to the current nomenclature (Fredholm et al., 1994). As expected, the kinetics and pharmacological properties of this response indicate that slow membrane

depolarization is not mediated by ligand-gated channels. *N*-ethylmaleimide which is known to uncouple receptors from G-proteins, inhibited this slow depolarization. Our results also indicated that inhibition of protein kinase activity with calphostin or staurosporine also prevented this depolarization. KT5720, a protein kinase A inhibitor, did not affect the ATP slow response at concentrations that inhibited the slow depolarization induced by adenosine. Previous experimental evidence indicate that the latter response is mediated by A2 adenosine receptors, and likely by adenyl cyclase and protein kinase A activity (Barajas-López, 1993, 1994). Furthermore, under the same experimental conditions used here, staurosporine, but not KT5720, inhibits the slow depolarization induced by a 12,13-dibutyrate, a protein kinase C activator (Barajas-López, 1993). These observations and the fact the slow depolarization induced by ATP appear to be associated with intracellular Ca^{2+} release suggests that diacylglycerol and protein kinase C might mediating the inhibition of the membrane K^+ conductance.

Both, ATP and adenosine can inhibit the membrane K^+ conductance in the S/type 1 submucosal neurons and cause depolarization (Barajas-López et al., 1991, 1994). Several observations indicate that these agonists act at different type of receptors which, however, are 8-cyclopentyltheophylline sensitive. Thus, the slow depolarization induced by ATP is seen even in neurons with no response to adenosine (Barajas-López et al., 1994). Metabolism of ATP to adenosine does not seem to contribute significantly to the ATP depolarization, since treatments which are known to inactivate adenosine (with adenosine deaminase) and prevent breakdown of ATP (with α,β-methylene ADP) had no effect on ATP responses (present study). In addition, the protein kinase A inhibitor KT5720 blocked the slow depolarization induced by the adenosine analog 2-chloroadenosine but did not affect that induced by ATP.

4.3. Calcium signaling

Our observations carried out during our Ca^{2+} studies are also in agreement with the sequential activation of P2X and P2Y receptors during the stimulation with ATP of submucosal neurons. Fast and slow Ca^{2+} responses were distinguished on the basis of their kinetics and their pharmacological profiles. Our findings suggest that the fast ATP Ca^{2+} transient is associated with fast membrane depolarization, and the slow Ca^{2+} transient is associated with the slow membrane depolarization. Thus, the 'fast' ATP Ca^{2+} and potential responses had certain characteristics in common: (1) short latencies less than 0.5 s, (2) inhibition by PPADS, (3) enhancement by suramin, (4) opposing effects of suramin and PPADS in the same submucosal neuron, and (5) lack of effect of staurosporine in cells which had PPADS-sensitive responses. On the other hand, the 'slow' Ca^{2+} response and the slow depolarization also had (1) similar latencies, (2) were not affected by PPADS, (3) but were inhibited by *N*-ethylmaleimide.

The lack of effect of Cd^{2+} on the slow ATP Ca^{2+} response at a concentration that is known to completely block voltage operated Ca^{2+} channels in enteric neurons (Barajas-López et al., 1996b) implies that these channels are not involved in the ATP-induced slow $[Ca^{2+}]_i$ transient. This feature also distinguishes this response from the fast $[Ca^{2+}]_i$ transient, which was inhibited by Cd^{2+} and by omitting Ca^{2+} ions from the extracellular fluid. However, Cd^{2+} only partially blocked the fast $[Ca^{2+}]_i$ transient, whereas the removal of the extracellular Ca^{2+} or blockade of P2X receptors with PPADS completely blocked it. These observations would imply that the fast rise in $[Ca^{2+}]_i$ is likely the result of Ca^{2+} influx through both P2X and voltage operated Ca^{2+} channels.

Collectively, the data supports the hypothesis that activation of P2Y leads to an initial inhibition of the membrane K^+ conductance mediated by protein kinase C activation, which induces a slow depolarization in the S/Type 1 submucosal neurons. Activation of P2Y receptors also induce a gradual rise in $[Ca^{2+}]_i$ which, however, does not required protein kinase C activation. Despite the fact that several different pools of Ca^{2+} could be mobilized in response to P2Y receptor activation, the simplest explanation for our results would be that such a pool is the one sensitive to inositol 1,4,5 trisphosphate (IP_3). Similar to that mobilized in myenteric neurons after activation of P2Y receptors and which are linked to the phospholipase C signaling pathway (Christofi et al., 1997). In other words, our hypothesis is that activation of P2Y receptors activate the phospholipase C, giving rise to IP_3 and diacylglycerol. IP_3 would induced the release of intracellular Ca^{2+} pools and would be responsible for the slow Ca^{2+} transient. The physiological role of Ca^{2+} in the slow depolarization remains to be elucidated. Diacylglycerol, on the other hand, would activated the protein kinase C (by a mechanism still to be determined) leading to a reduction in the membrane K^+ conductance and slow depolarization, as it was discussed above. In agreement with this hypothesis, it has been shown that P2Y is linked with the phospholipase C signaling pathway in numerous cells, including neurons (El-Moatassim et al., 1992).

Some mixed 'fast/slow' Ca^{2+} responses in which the initial fast response was followed by a slow response are reminiscent of the respective P2X-mediated fast depolarization and P2Y-mediated slow depolarizations observed in S/Type 1 neurons. Although this was not tested directly in our studies, it is consistent with our data showing that distinct pharmacological profiles exist for fast and slow responses. Multiple Ca^{2+} pools contribute to such complex purinergic Ca^{2+} transients. The spatial anomalies in the rise in $[Ca^{2+}]_i$ in submucous neurons argues for the contribution of multiple intracellular Ca^{2+} pools. Oscillations in $[Ca^{2+}]_i$ during the plateau phase of the ATP Ca^{2+} tran-

sient could be due to Ca^{2+} induced Ca^{2+} release, although this remains to be proven. In cultured guinea-pig myenteric neurons, oscillations in $[Ca^{2+}]_i$ via a Ca^{2+} induced Ca^{2+} release mechanism involves Ca^{2+} influx and a ryanodine/caffeine sensitive intracellular pool (Guan and Christofi, unpublished observations).

There is a clear delay in the occurrence of the Ca^{2+} response during both the fast and slow membrane depolarizations. For instance, the Ca^{2+} response occurs 300 ms after the onset of the fast depolarization, and 3 s after the onset of the slow depolarization. The length of the delay in the onset of the slow Ca^{2+} response is consistent with the slower activation of the phospholipase C signaling cascade. The brief delay in the onset of the fast Ca^{2+} response is in part explained by the requirement of an initial depolarization and activation of voltage operated Ca^{2+} channels.

Since intracellular recordings were not made from the same neurons in which Ca^{2+} was measured, the identity of the neurons in the latter response remains equivocal. A potential caveat is that some of the responsive neurons are AH/Type 2 neurons. In the myenteric plexus, these neurons display prominent ATP-induced hyperpolarizations believed to be due to a rise in $[Ca^{2+}]_i$ (Katayama and Morita, 1989; Christofi et al., 1997). This issue can directly be resolved in future studies by the combination of electrophysiology and fura-2 Ca^{2+} microfluorimetry (not available to us during the course of this study).

Not all S/Type 1 neurons had both fast and slow membrane depolarization responses. Furthermore, a subset of neurons displayed either a fast or a slow response. The type(s) of ATP Ca responses occurring in cultured submucosal neurons were equally as unpredictable; three subsets of cells could be distinguished: those with fast and slow responses, those with only fast responses and those with only slow responses. These data supports the hypothesis that three distinct functional subsets of S/Type 1 neurons exist in the submucous plexus under the influence of P2X, P2Y or both P2X and P2Y receptors. The great variance in the magnitude of ATP responses may in part, also be due to activation of a heterogeneous population of S/Type 1 neurons. If this hypothesis is true, different classes of S/Type 1 neurons with distinct ATP responses would be expected to vary in their morphology, projections and/or chemical coding; this warrants further study that could yield important information on the physiological role of P2X and P2Y receptors in the enteric nervous system.

In conclusion, the fast and slow depolarizations are mediated by activation of P2X and P2Y receptors, respectively. Ca^{2+} is a major intracellular signal for transduction of P2X and P2Y purinergic messages. Similar P2X receptors are present in both the submucosal (present study) and myenteric neurons (Barajas-López et al., 1996a) of the guinea-pig ileum, as suggested by the fact that the electrophysiological properties and pharmacological profile of these receptors are the same in neurons from both plexuses.

Acknowledgements

This work was supported by the Medical Research Council of Canada (grant #13491 to Carlos Barajas-López) and National Institutes of Health (grant #DK44179 to Fedias L. Christofi. Carlos Barajas-López was also supported by the Ontario Ministry of Health (Career Scientist Award #04500).

References

Barajas-López, C., 1993. Adenosine reduces the potassium conductance of guinea-pig submucosal plexus neurons by activating protein kinase A. Pfluegers Arch. 424, 410–415.

Barajas-López, C., 1994. Interactions between inhibitory and excitatory modulatory signals in single submucosal neurons. Am. J. Physiol. 267, C1359–C1365.

Barajas-López, C., Surprenant, A., North, R.A., 1991. Adenosine A1 and A2 receptors mediate presynaptic inhibition and postsynaptic excitation in guinea pig submucosal neurons. J. Pharmacol. Exp. Ther. 258, 490–495.

Barajas-López, C., Barrientos, M., Espinosa-Luna, R., 1993. Suramin increases the efficacy of ATP to activate an inward current in myenteric neurons from guinea pig ileum. Eur. J. Pharmacol. 250, 141–145.

Barajas-López, C., Espinosa-Luna, R., Gerzanich, V., 1994. ATP closes a potassium and opens a cationic conductance through different receptors in neurons of guinea-pig submucous plexus. J. Pharmacol. Exp. Ther. 268, 1396–1402.

Barajas-López, C., Muller, M.J., Prieto-Gómez, B., Espinosa-Luna, R., 1995. ATP inhibits the synaptic release of acetylcholine in submucosal neurons. J. Pharmacol. Exp. Ther. 274, 1238–1245.

Barajas-López, C., Huizinga, J.D., Collins, S.M., Gerzanich, V., Espinosa-Luna, R., Peres, A.L., 1996a. P2X-purinoceptors of myenteric neurones from the guinea-pig ileum and their unusual pharmacological properties. Br. J. Pharmacol. 119, 1541–1548.

Barajas-López, C., Peres, A.L., Espinosa-Luna, R., 1996b. Cellular mechanisms underlying adenosine actions on cholinergic transmission in enteric neurons. Am. J. Physiol. 271, C264–C275.

Barajas-López, C., Espinosa-Luna, R., Zhu, Y., 1998. Functional interactions between nicotinic and P2X channels in short-term cultures of submucosal neurons. J. Physiol. (London) 513, 671–683.

Bean, B.P., 1992. Pharmacology and electrophysiology of ATP-activated ion channels. TIPS 13, 87–90.

Buell, G., Lewis, C., Collo, G., North, R.A., Surprenant, A., 1996. An antagonist-insensitive P2X receptor expressed in epithelia and brain. EMBO J. 15, 55–62.

Burnstock, G., 1986. Autonomic neuromuscular junctions: current developments and future directions. J. Anat. 146, 1–30.

Christofi, F.L., Wood, J.D., 1994. Electrophysiological subtypes of inhibitory P1 purinoceptors on myenteric neurones of guinea-pig small bowel. Br. J. Pharmacol. 113, 703–710.

Christofi, F.L., Guan, Z., Wood, J.D., Baidan, L.V., Stokes, B.T., 1997. Purinergic Ca^{2+} signaling in myenteric neurons via P2 purinoceptors. Am. J. Physiol. 272, G463–G473.

Collo, G., North, R.A., Kawashima, E., Merlo-Pich, E., Neidhart, S., Surprenant, A., Buell, G., 1996. Cloning of P2X5 and P2X6 receptors and the distribution and properties of an extended family of ATP-gated ion channels. J. Neurosci. 16, 2495–2507.

Collo, G., Neidhart, S., Kawashima, E., Kosco-Vilbois, M., North, R.A., Buell, G., 1997. Tissue distribution of the P2X7 receptor. Neuropharmacology 36, 1277–1283.

Connolly, G.P., 1995. Differentiation by pyridoxal 5-phosphate, PPADS and IsoPPADS between responses mediated by UTP and those evoked by alpha, beta-methylene-ATP on rat sympathetic ganglia. Br. J. Pharmacol. 114, 727–731.

Edwards, F.A., Gibb, A.J., Colquhoun, D., 1992. ATP receptor-mediated synaptic currents in the central nervous system. Nature 359, 144–147.

El-Moatassim, C., Dornand, J., Mani, J.C., 1992. Extracellular ATP and cell signaling. Biochim. Biophys. Acta 1134, 31–45.

Evans, R.J., Surprenant, A., 1992. Vasoconstriction of guinea-pig submucosal arterioles following sympathetic nerve stimulation is mediated by the release of ATP. Br. J. Pharmacol. 106, 242–249.

Evans, R.J., Derkach, V., Surprenant, A., 1992. ATP mediates fast synaptic transmission in mammalian neurons. Nature 357, 503–505.

Fieber, L.A., Adams, D.J., 1991. Adenosine triphosphate-evoked currents in cultured neurones dissociated from rat parasympathetic cardiac ganglia. J. Physiol. (London) 434, 239–256.

Fredholm, B.B., Abbracchio, M.P., Burnstock, G., Daly, J.W., Harden, T.K., Jacobson, K.A., Leff, P., Williams, M., 1994. Nomenclature and classification of purinoceptors. Pharmacol. Rev. 46, 143–156.

Friel, D.D., 1988. An ATP-sensitive conductance in single smooth muscle cells from the vas deferens. J. Physiol. (London) 401, 361–380.

Friel, D.D., Bean, B.P., 1988. Two ATP-activated conductances in bullfrog atrial cells. J. Gen. Physiol. 91, 1–27.

Galligan, J.J., Bertrand, P.P., 1994. ATP mediates fast synaptic potentials in enteric neurons. J. Neurosci. 14, 7563–7571.

Grynkiewicz, G., Poenie, M., Tsien, R.Y., 1985. A new generation of Ca^{2+} indicators with greatly improved fluorescence properties. J. Biol. Chem. 260, 3440–3450.

Hirst, G.D.S., Holman, M.E., Spence, I., 1974. Two type of neurones in the myenteric plexus of duodenum in the guinea-pig. J. Physiol. (London) 236, 303–326.

Inoue, K., Nakazawa, K., Fujimori, K., Watano, T., Takanaka, A., 1992. Extracellular adenosine 5′-triphosphate-evoked glutamate release in cultured hippocampal neurons. Neurosci. Lett. 134, 215–218.

Katayama, Y., Morita, K., 1989. Adenosine 5′-triphosphate modulates membrane potassium conductance in guinea-pig myenteric neurones. J. Physiol. (London) 408, 373–390.

Kenakin, R., 1993. Pharmacologic Analysis of Drug-Receptor Interaction. Raven Press, New York.

Kennedy, C., Leff, P., 1995. How should P2X purinoceptors be classified pharmacologically? TIPS 16, 168–174.

Khakh, B.S., Humphrey, P.P.A., Surprenant, A., 1995. Electrophysiological properties of P2X-purinoceptors in rat superior cervical, nodose and guinea-pig coeliac neurones. J. Physiol. (London) 484, 385–395.

Kimball, B.C., Yule, D.I., Mulholland, M.W., 1996. Caffeine- and ryanodine-sensitive Ca^{2+} stores in cultured guinea pig myenteric neurons. Am. J. Physiol. 270, G594–G603.

Lewis, C., Neidhart, S., Holy, C., North, R.A., Buell, G., Surprenant, A., 1995. Coexpression of P2X2 and P2X3 receptor subunits can account for ATP-gated currents in sensory neurons. Nature 377, 432–435.

Nishi, S., North, R.A., 1973. Intracellular recording from the myenteric plexus of the guinea-pig ileum. J. Physiol. (London) 231, 471–491.

North, R.A., 1996. Families of ion channels with two hydrophobic segments. Curr. Opin. Cell Biol. 8, 474–483.

Nutter, T.J., Adams, D.J., 1994. Adenosine 5′-triphosphate receptor-mediated currents in rat intracardiac neurons. In: Belardinelli, A., Pelleg, A. (Eds.), Adenosine and Adenine Nucleotides. Martinus Nijboff, Boston, pp. 121–131.

Silinsky, E.M., Gerzanich, V., 1993. On the excitatory effects of ATP and its role as a neurotransmitter in coeliac neurons of the guinea-pig. J. Physiol. (London) 464, 197–212.

Soto, F., Garcia-Guzman, M., Gomez-Hernandez, J.M., Hollmann, M., Karschin, C., Stuhmer, W., 1996. P2X4: an ATP-activated ionotropic receptor cloned from rat brain. Proc. Natl. Acad. Sci. U. S. A. 93, 3684–3688.

Valera, S., Hussy, N., Evans, R.J., Adami, N., North, R.A., Surprenant, A., Buell, G., 1994. A new class of ligand-gated ion channel defined by P2X receptor for extracellular ATP. Nature 371, 516–519.

Windscheif, U., Ralevic, V., Baumert, H.G., Mutschler, E., Lambrecht, G., Burnstock, G., 1994. Vasoconstrictor and vasodilator responses to various agonists in the rat perfused mesenteric arterial bed: selective inhibition by PPADS of contractions mediated via P2X-purinoceptors. Br. J. Pharmacol. 113, 1015–1021.